AJNR

MR Line Scan Diffusion Imaging of the Brain in Children

Richard L. Robertson, Stephan E. Maier, Caroline D. Robson, Robert V. Mulkern, Palagia M. Karas and Patrick D. Barnes

AJNR Am J Neuroradiol 1999, 20 (3) 419-425
http://www.ajnr.org/content/20/3/419

AJNR Am J Neuroradiol 20:419–425, March 1999

MR Line Scan Diffusion Imaging of the Brain in Children

Richard L. Robertson, Stephan E. Maier, Caroline D. Robson, Robert V. Mulkern, Palagia M. Karas, and Patrick D. Barnes

BACKGROUND AND PURPOSE: **MR imaging of the self-diffusion of water has become increasingly popular for the early detection of cerebral infarction in adults. The purpose of this study was to evaluate MR line scan diffusion imaging (LSDI) of the brain in children.**

METHODS: **LSDI was performed in four volunteers and 12 patients by using an effective TR/TE of 2736/89.4 and a maximum *b* value of 450 to 600 s/mm^2 applied in the *x*, *y*, and *z* directions. In the volunteers, single-shot echo planar imaging of diffusion (EPID) was also performed. The patients (10 boys and two girls) ranged in age from 2 days to 16 years (average age, 6.6 years). Diagnoses included acute cerebral infarction, seizure disorder, posttraumatic confusion syndrome, complicated migraine, residual astrocytoma, encephalitis, hypoxia without cerebral infarction, cerebral contusion, and conversion disorder. In all patients, routine spin-echo images were also acquired. Trace images and apparent diffusion coefficient maps were produced for each location scanned with LSDI.**

RESULTS: **In the volunteers, LSDI showed less chemical-shift and magnetic-susceptibility artifact and less geometric distortion than did EPID. LSDI was of diagnostic quality in all studies. Diffusion abnormalities were present in five patients. Restricted diffusion was present in the lesions of the three patients with acute cerebral infarction. Mildly increased diffusion was present in the lesions of encephalitis and residual cerebellar astrocytoma. No diffusion abnormalities were seen in the remaining seven children.**

CONCLUSION: **LSDI is feasible in children, provides high-quality diffusion images with less chemical-shift and magnetic-susceptibility artifact and less geometric distortion than does EPID, and complements the routine MR examination.**

MR imaging of the self-diffusion of water has become increasingly popular in recent years, particularly for the early detection of cerebral infarction in adults with acute ischemic stroke (1–4). Preliminary experience in the evaluation of diffusion abnormalities in hypoxic-ischemic injury of the neonate has also been reported (5). Additionally, diffusion-weighted MR imaging has been used to differentiate cytotoxic from vasogenic edema associated with signal abnormality on T2-weighted spin-echo (SE) MR images, to evaluate the developing brain, and to assess neoplastic and demyelinating disorders (6–10).

Received June 19, 1998; accepted after revision November 23.

From the Department of Radiology, Children's Hospital Medical Center and Harvard Medical School (R.L.R., C.D.R., R.V.M., P.M.K., P.D.B.); and the Department of Radiology, Brigham and Women's Hospital and Harvard Medical School (S.E.M.), Boston.

Address reprint requests to Richard L. Robertson, MD, Department of Radiology, Children's Hospital Medical Center, 300 Longwood Ave, Boston, MA 02115.

The initial attempts at in vivo diffusion-weighted MR imaging were subject to bulk motion, which made images prone to artifacts (11). The development of single-shot echo-planar imaging of diffusion (EPID) largely overcame these limitations (12). EPID, however, requires specialized hardware that is not widely available at present. EPID also suffers from chemical-shift and magnetic-susceptibility artifacts as well as geometric distortion. This makes interpretation of the images difficult and may obscure lesions near the skull base or next to metallic implants.

To overcome the difficulties inherent in EPID, non-EPI–based techniques have been developed, including half-Fourier single-shot turbo SE (HASTE) and navigated SE diffusion-weighted MR imaging (3, 13). Another technique recently proposed is line scan diffusion imaging (LSDI) (14).

LSDI uses multiple diffusion-weighted SE column excitations to create a two-dimensional image. Because the individual columns of data are collected independently, LSDI is relatively insensitive to motion. Furthermore, since the technique is SE

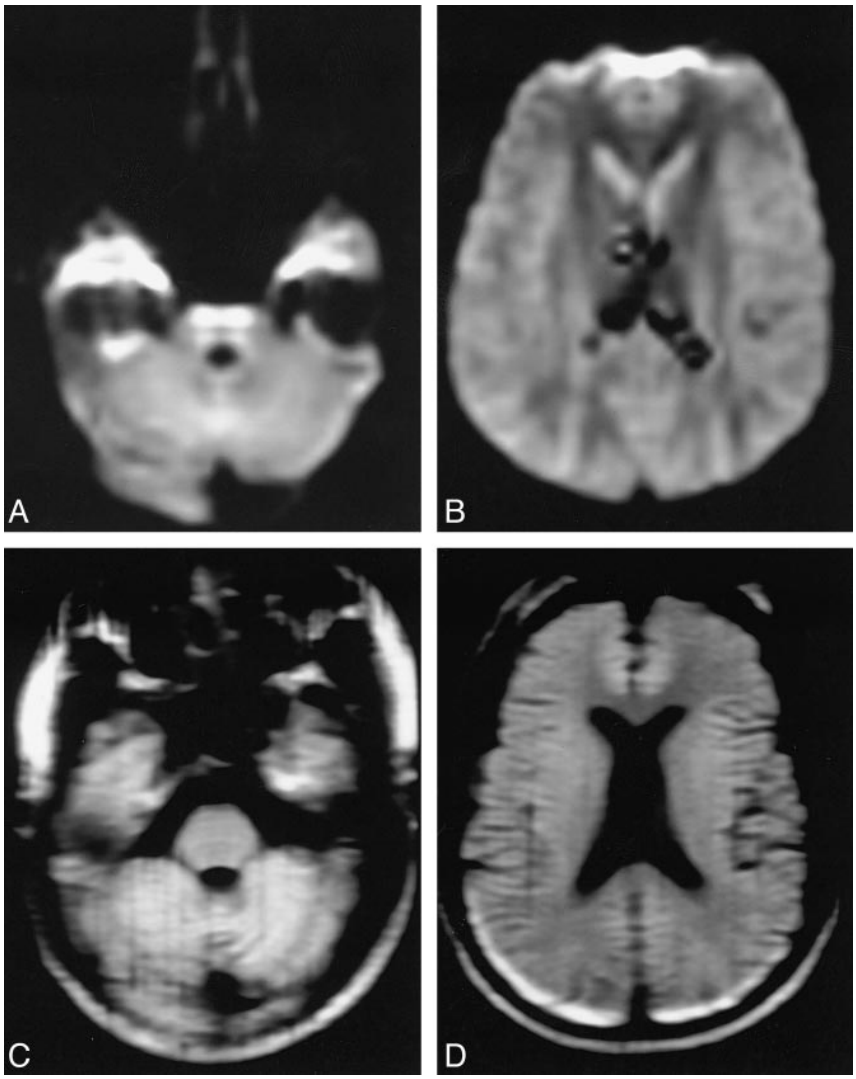

FIG 1. EPID versus LSDI in a healthy volunteer.

A and *B,* EPID (2000/90/1; b = 600 s/mm^2) trace images at two anatomic levels show geometric distortion of the brain stem and artifactual high signal intensity in the temporal lobes and anterior frontal lobes.

C and *D,* LSDI (2736/89/1; b = 600 s/mm^2) trace images at corresponding levels show less geometric distortion and less magnetic-susceptibility artifact.

based, magnetic-susceptibility artifacts and geometric distortion are minimized (15). Unlike HASTE and navigated SE diffusion-weighted imaging, LSDI performs well without the use of cardiac gating or head restraints (3, 13, 14). These properties should make LSDI a useful sequence for the evaluation of pediatric neurologic diseases.

Methods

Volunteers

For the purposes of comparing LSDI with EPID, four volunteers, including one with a ventricular shunt catheter and one with dental braces, were evaluated with both LSDI and EPID (Figs 1 and 2). For one of the normal studies (Fig 2), a paper clip was taped to the subject's forehead during both the LSDI and EPID examinations. Masking tape was placed over the skin and under the clip to reduce the potential for radiofrequency pulse--induced burns.

Patients

Twelve patients, 10 boys and two girls, underwent LSDI in addition to conventional and fast SE brain MR imaging (see Table). The patients ranged in age from 2 days to 16 years (average age, 6.5 years). Four of the patients were newborns. One patient underwent two imaging studies. Diagnoses included acute stroke (n = 3), seizure disorder (n = 2), posttraumatic confusion syndrome (n = 1), complicated migraine (n = 1), residual astrocytoma (n = 1), encephalitis (organism not isolated) (n = 1), hypoxia due to pneumonia without cerebral infarction (n = 1), cerebral contusion (n = 1), and conversion disorder (n = 1). The MR studies were performed between 8 hours and 14 days after the onset of symptoms (see Table). CT studies were performed in nine patients 2 to 72 hours (average, 35 hours) before the MR studies. Two patients were studied with conventional angiography. Clinical follow-up ranged from 3 to 12 weeks.

MR Protocol

The MR protocol included T1-weighted conventional SE, T2-weighted fast SE, fluid-attenuated inversion recovery (FLAIR), and LSDI sequences in all 12 patients. All MR studies were performed on a 1.5-T imaging system with a quadrature head coil. From August to November 1997, the system was equipped with standard gradient hardware; since November 1997, the gradient hardware has been capable of EPI.

MR Parameters

MR imaging was performed using conventional SE sagittal T1-weighted images (600/20/2 [TR/TE/excitations]; 20- to 24-

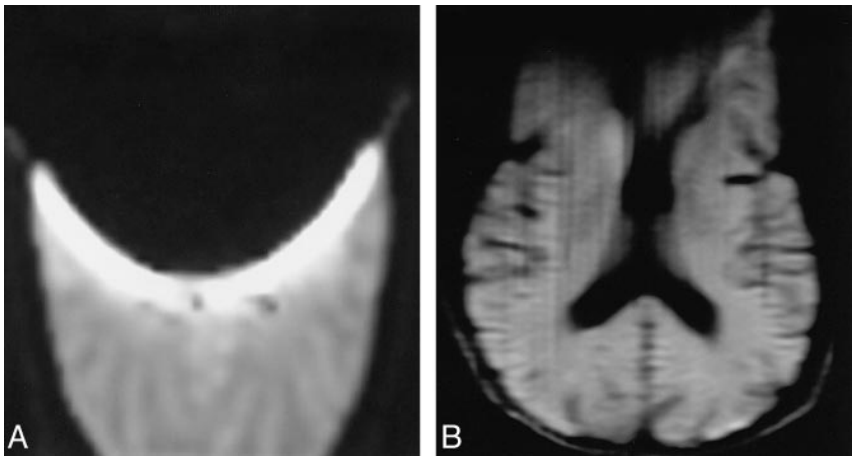

FIG 2. EPID versus LSDI in a volunteer with a paper clip taped to the forehead.

A, EPID (2000/90/1; b = 600 s/mm^2) trace image shows marked signal loss due to magnetic-susceptibility effect in the anterior two thirds of the brain.

B, LSDI (2736/89/1; b = 600 s/mm^2) trace image at the same level shows less artifactual signal loss with preservation of much of the anatomic detail.

cm field of view, 5-mm section thickness with a 20% intersection gap, and 256 × 192 acquisition matrix); fast SE T2-weighted images ($3200/85_{eff}$/1, 24-cm field of view, 5-mm section thickness with a 20% intersection gap, 256 × 192 acquisition matrix, and echo train length = 8); and FLAIR fast SE images ($10002/162_{eff}$/1, TI = 2200, 24-cm field of view, 5-mm section thickness with a 20% intersection gap, and 256 × 192 acquisition matrix).

LSDI Parameters

The LSDI technique has been described previously (14). LSDI was performed at six axial locations using an effective TR/TE of 2736/89.4, 1 excitation, 20- × 15-cm field of view, effective section thickness of 7 mm (14, 15) with a 20% to 29% intersection gap, 128 × 160 acquisition matrix, and b = 0 and 450 to 600 s/mm^2 with the maximum b value applied in the x, y, and z directions. The total imaging time was 7 minutes 54 seconds. Trace images and apparent diffusion coefficient (ADC) maps were produced for each of the six locations off-line.

EPID Parameters

The EPID sequence was performed at anatomic locations corresponding to the levels imaged by LSDI. The following parameters were used: 2000/90/1, 40- × 20-cm field of view, single-shot technique, 7-mm section thickness with a 29% gap, 128 × 64 matrix, and b = 0 and 600 s/mm^2, x, y, and z directions. The total imaging time was 8 seconds. Trace and ADC maps were produced for each anatomic level. Signal-to-noise ratios (SNR) were calculated with noise sampled in both the phase- and frequency-encode directions for the EPID and LSDI images in the volunteers. Image quality and resolution of detail were compared between the LSDI and EPID images.

Images of only the supratentorial brain were obtained in seven patients. In five patients (six examinations), images of both the infratentorial and supratentorial brain were obtained.

Magnetic-susceptibility artifacts and geometric distortion were evaluated separately in the posterior fossa and temporal lobes and were graded by two independent observers as absent, minimal, moderate, or severe. Lesion ADC measurements were made from 1.0 cm^3 regions of interest (ROI) and compared with the corresponding location in the contralateral hemisphere to determine if the lesion had increased or restricted diffusion. Ratios of lesion ADC to normal tissue ADC were calculated. Lesion conspicuity was evaluated by measuring 1.0 cm^3 ROI measurements made of the lesion versus the surrounding normal brain parenchyma on both the T2-weighted (b = 0 s/mm^2) and trace (b = 450–600 s/mm^2) images.

Results

Volunteers

In the four subjects imaged with LSDI and EPID, LSDI images clearly showed fewer magnetic-susceptibility artifacts and less geometric distortion than did the EPID images (Figs 1 and 2). The SNR of the LSDI images was greater than that of the EPID images, whether the noise was measured in either the phase-encode or frequency-encode direction. LSDI images exhibited greater resolution of detail than did the EPID images.

Patients

Of the 10 patients in whom acute stroke was an initial clinical concern, three patients were determined to have cerebral infarction (cases 1, 6, and 8) whereas in the remaining seven patients the neurologic symptoms were ultimately attributed to other disorders (see Table). Definite or suspected density abnormalities were detected on CT studies in four patients (see Table). In one patient (case 12), a suspected lesion in the left internal capsule was not corroborated on MR studies. Parenchymal signal intensity abnormalities were present on the FLAIR and T2-weighted images on seven examinations in six patients.

LSDI was of diagnostic quality in all examinations (70 of 72 anatomic sections). In two patients, an image at one anatomic level was significantly degraded by patient motion. Images through the posterior fossa and temporal lobes showed minimal or no magnetic-susceptibility artifacts in all cases. Geometric distortion was not apparent on any of the images.

ADC abnormalities were present on six examinations in five patients (Figs 3–5). A focally decreased ADC was evident in the areas of cerebral infarction in the three patients with acute stroke. The measured ADC in these lesions was 48% to 66% (average, 58%) of the ADC of the contralateral normal structure. Abnormalities were present

Clinical data and MR findings in 12 children studied with line scan diffusion imaging (LSDI)

Case	Age	Symptoms	Diagnosis	Outcome	Time to CT/MR	Imaging Findings		
						CT	FLAIR and T2-Weighted	LSDI
1	2 d	Seizures, cyanosis	Stroke, hypoplastic L heart	Seizures controlled with medication	NA/36 h	NA	R frontal and bilateral parietal high signal	R frontal, R parietal and L frontal restricted diffusion
2	5 d	Seizures	Seizures, unknown origin	Continued seizures	5 h/36 h	Normal	Normal	Normal
3	7 d	Seizures	Seizures, unknown origin	Seizures controlled with medication	6 h/5 d	Normal	Normal	Normal
4	5 wk	Cyanosis, lethargy	Hypoxia due to pneumonia	Asymptomatic	36 h/72 h	Normal	Normal	Normal
5	23 mo	Seizures	Encephalitis	Asymptomatic	28 h/52 h	Normal	High signal, R thalamus	Minimally increased diffusion, R thalamus
6	5 y	L hemiparesis	Stroke, varicella vasculitis	Mild L hemiparesis	20 h/24 h	Low density, R BG	High signal, R BG	Restricted diffusion, R BG
7	10 y	Comatose	Contusions, motor vehicle accident	Awake, not oriented	10 d/11 d	R temporal contusion	R temporal contusion	No diffusion abnormality
8	11 y	R hemiparesis	Strooke, L vertebral artery dissection	Mild R hemiparesis	24 h/48 h	Low density, L IC	Hyperintensity, L IC	Restricted diffusion, L IC
		Vertical diplopia	TIA	Diplopia resolved	NA/12 h	NA	No new lesions, L IC cavity	No new lesions, increased diffusion, L IC
9	13 y	Ataxia	Cerebellar asctrocytoma	Ataxia	NA/14 d	NA	Residual tumor, R cerebellum	Minimally increased diffusion in residual tumor
10	14 y	Headache, aphasia	Complicated migraine	Symptoms resolved	6 h/12 h	Normal	Normal	Normal
11	14 y	R arm tingling	Conversion disorder	Symptoms resolved	NA/10 h	NA	Normal	Normal
12	16 y	Headache, confusion	Posttraumatic confusion syndrome	Symptoms resolved	6 h/8 h	? Hypodensity, L IC	Normal	Normal

Note.—FLAIR indicates fluid-attenuated inversion recovery; NA, not available; BG, basal ganglia; TIA, transient ischemic attack; IC internal capsule.

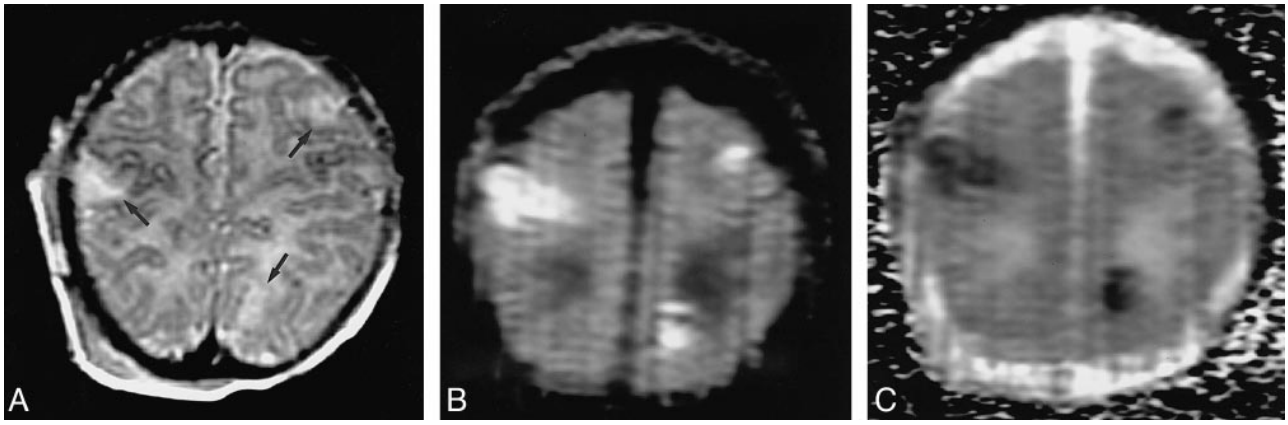

FIG 3. Case 1: Neonate with hypoplastic left heart and seizures due to embolic infarction.
A, Three hyperintense lesions (*arrows*) are evident on the T2-weighted (3200/85/1) image.
B, The lesions are more conspicuous on the LSDI (2736/89/1; $b = 600$ s/mm^2) trace image.
C, The lesions have decreased ADCs, as shown by low intensity on the diffusion map.

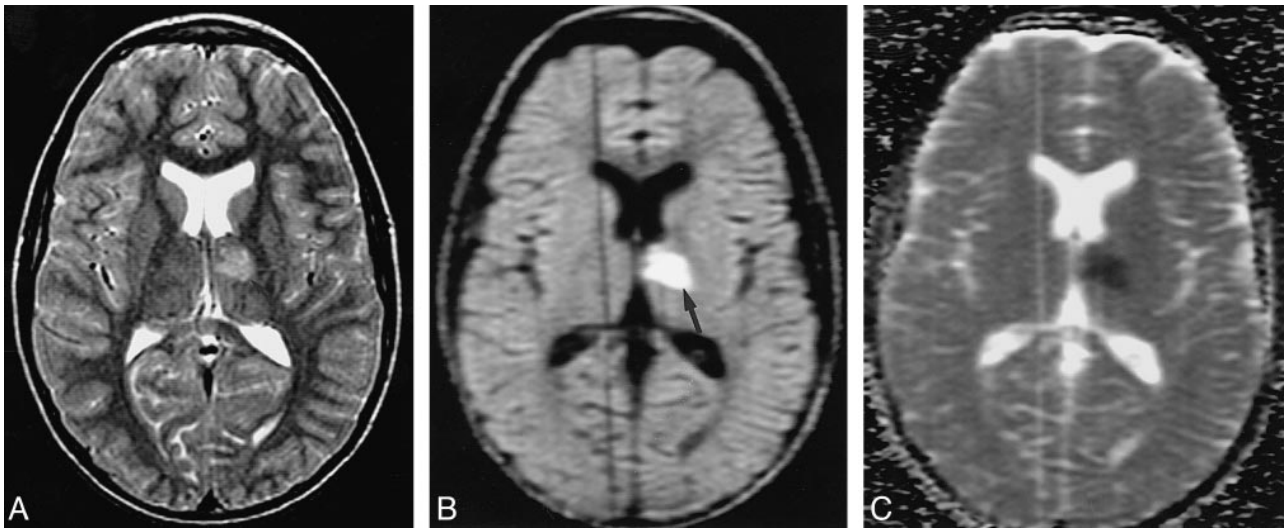

FIG 4. Case 8: 11 year-old boy with new left hemiparesis due to emboli from a vertebral artery dissection.
A–C, A left thalamocapsular lesion is evident on the T2-weighted (3200/85/1) image (*arrow, A*). The lesion is more conspicuous on the LSDI (2736/89/1; $b = 600$ s/mm^2) trace image (*arrow, B*), and has a decreased ADC on the diffusion map (*C*), indicating an acute infarction.

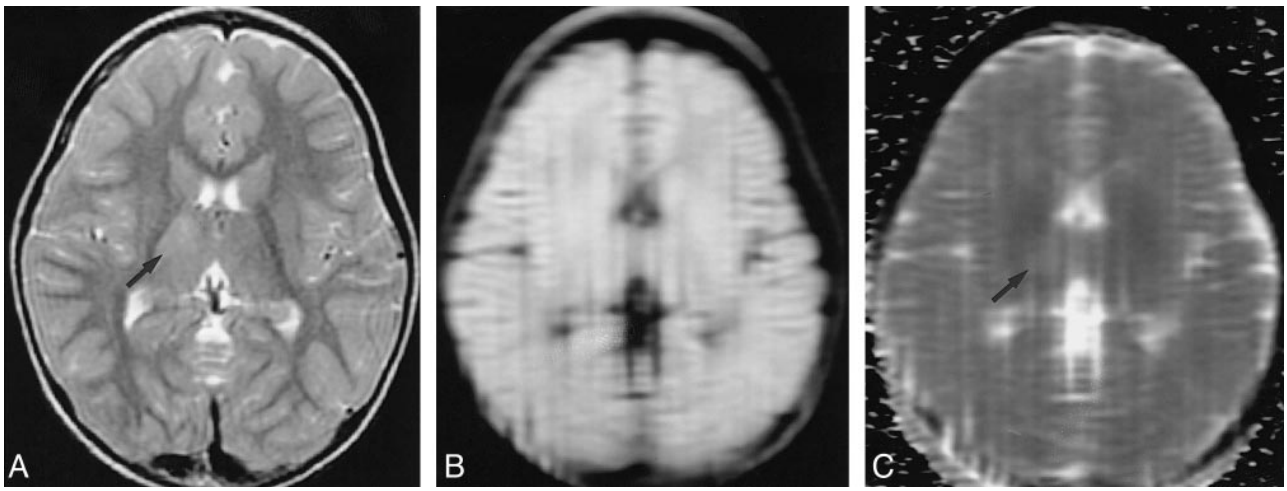

FIG 5. Case 5: 2-year-old girl with left-sided body seizures due to encephalitis.
A–C, A minimally hyperintense lesion is present in the right thalamus on the T2-weighted (3200/85/1) image (*arrow, A*). The lesion is nearly isointense on the LSDI (2736/89/1; $b = 600$ s/mm^2) trace image (*B*), and has a slightly increased ADC on the ADC map (*arrow, C*), as indicated by mildly increased signal. The increased ADC confirms that this is not an acute infarction.

on the T2-weighted images in all these patients. In one patient (case 8) who underwent a follow-up MR examination at 1 month, the lesion with restricted diffusion on the initial image exhibited increased diffusion corresponding to cavitation on the T2-weighted images. A mildly increased ADC (12% greater than normal brain) was present in the lesion in the patient with encephalitis (case 5, Fig 5) and in the residual tumor (10% greater than the normal cerebellum) in the patient with cerebellar astrocytoma (case 13).

Lesion conspicuity as determined by ROI measurements was greater on the LSDI trace (isotropic $b = 450$ or 600 s/mm^2) images (lesion signal intensity 177% to 199% of surrounding tissue) than on the T2-weighted ($b = 0$ s/mm^2) images (lesion signal intensity 126% to 142% of surrounding tissue) in all acute cerebral infarctions (Figs 3 and 4).

Discussion

The use of diffusion-weighted imaging for the early detection of stroke in adults has attained significant clinical relevance (1–3, 11, 13, 15, 16). In the pediatric patient, potential applications of diffusion-weighted imaging include the early demonstration of cerebral infarction due to hypoxia-ischemia or focal cerebrovascular occlusion, the differentiation of ischemic from nonischemic lesions, and the evaluation of brain development.

In the newborn or very young infant, the symptoms and signs of a stroke are often nonspecific (eg,

seizure or irritability), and cerebral infarction is only one of a variety of potential causes. Earlier and more accurate demonstration of infarctions is therefore desirable. Using conventional MR imaging, ischemic brain lesions are frequently difficult to identify during the first few days of life owing to the relatively high water content of the neonatal brain. Because of the extremely high water content of the preterm brain, the delineation of cerebral infarctions is especially difficult in these infants. However, with diffusion-weighted MR imaging, the high diffusibility of extracellular water renders a low background signal intensity against which ischemic lesions with cytotoxic edema and restricted diffusion are readily apparent (Fig 3). Therefore, the use of diffusion-weighted imaging should enable a significant improvement in the detection and diagnosis of neonatal stroke.

Cerebral infarctions are uncommon events in older children and there is often a delay in the diagnosis of stroke. Consequently, abnormalities are frequently present on T2-weighted MR sequences when patients are first imaged. The value of diffusion-weighted imaging in this setting is the greater specificity in the evaluation of intensity abnormalities evident on the conventional images. In our patients with abnormalities on T2-weighted sequences, diffusion-weighted imaging assisted in differentiating ischemic lesions (restricted diffusion; eg, cases 1, 6, and 8) from nonischemic lesions (increased diffusion; eg, case 5) lesions. The ability to differentiate ischemic from nonischemic lesions in children with acute neurologic deficits helps to identify those patients in whom additional or more invasive testing, such as cerebral angiography, is required for diagnosis. Alternatively, negative findings on diffusion-weighted and conventional MR examinations provide evidence that the patient's symptoms are due to causes other than acute cerebral infarction (eg, cases 2, 3, 4, 10, 11, and 12).

Diffusion tensor imaging (DTI) has been used to evaluate brain maturation in newborns and infants (17, 18). With the use of DTI, quantitative measures of both ADC and relative diffusion anisotropy can be obtained. Diffusion anisotropy refers to the observation of ADC variability when measured along different axes of a sample. Anisotropy is related to a variety of factors, including axon orientation and degree of myelination (19). As the brain matures, ADC decreases and there is an overall increase in diffusion anisotropy (18). DTI can therefore be used to study normal brain maturation as well as to evaluate the alterations in development that occur as a consequence of insults, such as cerebral ischemia or infection.

A variety of techniques for performing diffusion-weighted MR imaging are now available, including EPID, navigated SE diffusion-weighted imaging, HASTE diffusion-weighted imaging, and LSDI (3, 12–14). Each of these techniques has relative strengths and weaknesses in providing information about water diffusion in pediatric diseases of the CNS.

EPID is the fastest technique and minimizes motion artifacts, making quantitative diffusion measurements possible. High-quality EPID of the entire brain may be performed in less than 1 minute. However, EPID requires specialized hardware and software, which limit its availability. EPID is also associated with chemical-shift and magnetic-susceptibility artifacts as well as geometric distortion. These artifacts are most noticeable on images near the skull base and adjacent to metallic implants (Fig 1) and may make lesion detection and correlation with SE images in these regions difficult.

Navigated SEDI is a non-EPI–based diffusion sequence. This is a double-echo SE sequence in which a second non–phase-encoded navigator echo is used to correct for motion-induced phase shifts caused by the first imaging echo (13, 20). This technique requires cardiac gating and takes approximately 21 minutes to acquire a data set containing three maximum *b* value directions. This extremely long acquisition time is undesirable in the sedated or very ill child.

HASTE diffusion-weighted images are produced by using a half-Fourier single-shot turbo SE sequence. Whole-brain imaging can be performed in approximately 4 minutes for three *b* directions but the HASTE images have lower SNR and more image blur as compared with EPID images (3). HASTE imaging, like navigated SEDI, requires cardiac gating.

LSDI uses multiple diffusion-weighted SE column excitations to form a two-dimensional image (14). Because the images are constructed column by column, the technique is relatively insensitive to motion, as the time for the individual column acquisition is approximately equal to the TE. The use of a direct excitation of selected columns in a single shot avoids the use of phase-encoding multiple signal acquisitions from the entire plane each TR period, thereby minimizing sensitivity to macroscopic motion (14, 21). LSDI, therefore, does not require cardiac gating. Macroscopic motion during the acquisition of a given column results in loss of signal from that column of data while the remainder of the image is unaffected. Therefore, motion during acquisition of one or several columns does not significantly degrade the final trace image, which is a composite image of the three different *b* direction images. The insensitivity of LSDI to motion was evident in our patients, in whom only two anatomic sections were judged to be significantly degraded by motion artifacts. In our series, it was possible in all patients to acquire diagnostic LSDI images without the use of special head restraints apart from the normal padding used for routine scanning. LSDI did not require additional patient sedation or anesthesia beyond that already necessary for the routine MR imaging examination.

The relative lack of magnetic-susceptibility artifact and chemical-shift artifact with LSDI is a sig-

nificant advantage of this technique. The reduced magnetic-susceptibility artifact of LSDI compared with EPID is particularly helpful in imaging patients who have metallic implants, such as dental braces or ventricular shunt catheter reservoirs, as the artifacts from these devices severely degrade the EPID images.

Another advantage of LSDI over EPID is its lack of geometric distortion. The absence of distortion on LSDI images allows for easier and more precise comparison of the diffusion images and the routine anatomic images. The ability to accurately compare the diffusion and anatomic images may be beneficial in evaluating lesions with regional signal intensity variation, such as tumors or hemorrhages.

In our volunteers who underwent both EPID and LSDI, the LSDI images had a higher SNR and less image blur. The superior image detail and higher SNR of LSDI are additional advantages over the other available diffusion-weighted imaging techniques and make LSDI particularly well suited to performing DTI in the neonate (18).

A disadvantage of LSDI in the current protocol is the relatively long scan time. In our patients, we acquired six axial images with three maximum *b* directions in 7 minutes 54 seconds. A lower acquisition matrix of 128 × 92 would have yielded the same spatial resolution in approximately 60% of this scan time but would require off-line reconstruction and consequently would delay clinical interpretation. Therefore, for the purposes of on-line display of undistorted images, the 128 × 160 matrix option was selected. This is not a fundamental limitation, since integration of the off-line reconstruction with the scanner software is in principle possible. Nevertheless, further reductions of scan times are desirable for more complete coverage, since symptoms and signs of neurologic disease may be nonlocalizing, especially in the neonate or infant. Recently, a double-echo LSDI technique has been described that would reduce the image acquisition time by half (22). Acquiring images with a single-direction maximum *b* value would also reduce the total scan time by half, but the resulting anisotropy in the image would make scan interpretation more problematic. Since the patients in our series often had high-signal-intensity lesions on T2-weighted images with ''shine-through'' on diffusion-weighted images, the ability to map the ADC was essential in these patients for determining whether a true-diffusion abnormality was present. Therefore, the acquisition of a maximum *b* value in at least three directions is optimal.

Conclusion

LSDI is feasible for use in children and does not require cardiac gating, head restraints, or specialized hardware. LSDI is insensitive to macroscopic motion and provides high-quality diffusion images with less chemical-shift and magnetic-susceptibility artifact and less geometric distortion than does EPID. The length of the LSDI examination is longer than a comparable EPID sequence; however, methods for reducing LSDI scan times are in progress. The information obtained with LSDI is complementary to that provided by the conventional MR imaging study.

References

1. Chien D, Kwong K, Gress DR, et al. **MR diffusion imaging of cerebral infarction in humans.** *AJNR Am J Neuroradiol* 1992; 13:1097–1102
2. Moseley ME, Kucharczyk J, Mintorovitch J, et al. **Diffusion-weighted MR imaging of acute stroke: correlation with T2-weighted and magnetic susceptibility enhanced MR imaging in cats.** *AJNR Am J Neuroradiol* 1990;11:423–429
3. Lovblad K, Jakob PM, Chien Q, et al. **Turbo spin-echo diffusion-weighted MR of ischemic stroke.** *AJNR Am J Neuroradiol* 1998; 19:201–208
4. Bruning R, Wu RH, Deimling M, et al. **Diffusion measurements in the ischemic human brain with a steady-state sequence.** *Invest Radiol* 1996;31:709–715
5. Cowan FM, Pennock JM, Hanrahan JD, et al. **Early detection of cerebral infarction and hypoxic ischemic encephalopathy in neonates using diffusion-weighted magnetic resonance imaging.** *Neuropediatrics* 1994;25:172–175
6. Horsfield MA, Lai M, Webb SL, et al. **Apparent diffusion coefficients in benign and secondary progressive multiple sclerosis by nuclear magnetic resonance.** *Magn Reson Med* 1996; 36:393–400
7. Le Bihan D, Douek P, Argyropoulou M, et al. **Diffusion and perfusion magnetic resonance imaging in brain tumors.** *Top Magn Reson Imaging* 1993;5:25–31
8. Nomura Y, Sakuma H, Takeda K, et al. **Diffusional anisotropy of the human brain assessed with diffusion-weighted MR: relation with normal brain development and aging.** *AJNR Am J Neuroradiol* 1994;15:231–238
9. Toft PB, Leth H, Peitersen B, et al. **The apparent diffusion coefficient of water in gray and white matter of the infant brain.** *J Comput Assist Tomogr* 1996;20:1006–1011
10. Schaefer PW, Buonanno FS, Gonzalez RG, et al. **Diffusion-weighted imaging discriminates between cytotoxic and vasogenic edema in a patient with eclampsia.** *Stroke* 1997;28:1082–1085
11. Le Bihan D, Breton E, Lallemand D, et al. **MR imaging of intravoxel incoherent motions: application to diffusion and perfusion in neurologic disorders.** *Radiology* 1986;161:401–407
12. Turner R, Le Bihan D, Maier J et al. **Echo-planar imaging of intravoxel incoherent motions.** *Radiology* 1990;177:407–414
13. Marks MP, De Crespigny A, Lentz D, et al. **Acute and chronic stroke: navigated spin-echo diffusion weighted MR imaging.** *Radiology* 1996;199:403–408
14. Gudbjartsson H, Maier SE, Mulkern RV, et al. **Line scan diffusion imaging.** *Magn Reson Med* 1996;36:509–519
15. Maier SE, Gubdjartsson H, Patz S, et al. **Line scan diffusion imaging: characterization in healthy subjects and stroke patients.** *AJR Am J Roentgenol* 1998;171:85–93
16. Lutsep HL, Albers GW, DeCrespigny A, et al. **Clinical utility of diffusion-weighted magnetic resonance imaging in the assessment of ischemic stroke.** *Ann Neurol* 1997;41:574–580
17. Neil JJ, Shiran SI, McKinstry RC, et al. **Normal brain in human newborns: apparent diffusion coefficient and diffusion anisotropy measured by using diffusion tensor MR imaging.** *Radiology* 1998;209:57–66
18. Huppi PS, Maier SE, Peled S, et al. **Microstructural development of human newborn cerebral white matter assessed in vivo by diffusion tensor magnetic resonance imaging.** *Pediatr Res* 1998;44:584–590
19. Neill J. **Measurement of water motion (apparent diffusion) in biological systems.** *Concepts Magn Reson* 1997;9:385–401
20. Ordidge RJ, Helpern JA, Qing ZX, et al. **Correction of motion artifacts in diffusion-weighted MR images using navigator echoes.** *Magn Reson Imaging* 1994;12:455–460
21. Schwartz RB, Mulkern RV, Gubdjartsson H, et al. **Diffusion-weighted MR imaging in hypertensive encephalopathy: clues to pathogenesis.** *AJNR Am J Neuroradiol* 1998;19:859–862
22. Gudbjartsson H, Maier SE, Jolesz FA. **Double line scan diffusion imaging.** *Magn Reson Med* 1997;38:101–109